Polymorph-specific distribution of binding sites determines thioflavin-T fluorescence intensity in -synuclein fibrils

Sidhu, Arshdeep; Vaneyck, Jonathan; Blum, Christian; Segers-Nolten, Ine; Subramaniam, Vinod

published in
Amyloid : the international journal of experimental and clinical investigation : the official journal of the International Society of Amyloidosis

2018

DOI (link to publisher)
10.1080/13506129.2018.1517736

document version
Publisher's PDF, also known as Version of record

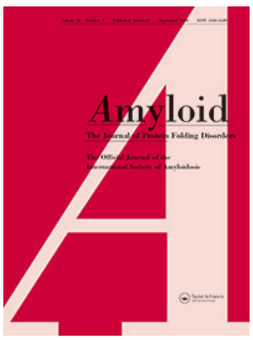

Taylor & Francis
Taylor & Francis Group

Amyloid
The Journal of Protein Folding Disorders

ISSN: 1350-6129 (Print) 1744-2818 (Online) Journal homepage: https://www.tandfonline.com/loi/iamy20

Polymorph-specific distribution of binding sites determines thioflavin-T fluorescence intensity in α-synuclein fibrils

Arshdeep Sidhu, Jonathan Vaneyck, Christian Blum, Ine Segers-Nolten & Vinod Subramaniam

To cite this article: Arshdeep Sidhu, Jonathan Vaneyck, Christian Blum, Ine Segers-Nolten & Vinod Subramaniam (2018) Polymorph-specific distribution of binding sites determines thioflavin-T fluorescence intensity in α-synuclein fibrils, Amyloid, 25:3, 189-196, DOI: 10.1080/13506129.2018.1517736

To link to this article: https://doi.org/10.1080/13506129.2018.1517736

AMYLOID
2018, VOL. 25, NO. 3, 189–196
https://doi.org/10.1080/13506129.2018.1517736

Taylor & Francis
Taylor & Francis Group

ORIGINAL ARTICLE

Polymorph-specific distribution of binding sites determines thioflavin-T fluorescence intensity in α-synuclein fibrils

Arshdeep Sidhu[a]*, Jonathan Vaneyck[a], Christian Blum[a], Ine Segers-Nolten[a] and Vinod Subramaniam[a,b]

[a]Nanobiophysics, MESA + Institute for Nanotechnology, University of Twente, Enschede, The Netherlands; [b]Executive Board, Vrije Universiteit Amsterdam, Amsterdam, The Netherlands

ABSTRACT

Thioflavin-T (ThT) is the most commonly used fluorescent dye for following amyloid formation semi-quantitatively *in vitro*, specifically probing the fibrillar cross-β-sheet content. In recent years, structural polymorphism of amyloid fibrils has been shown to be an important aspect of amyloid formation, both *in vitro* and in neurodegenerative diseases. Therefore, understanding ThT–amyloid interactions in the context of structural polymorphism of amyloids is necessary for correct interpretation of ThT fluorescence data. Here we study the influence of fibril morphology on ThT fluorescence and ThT binding sites, with two morphologically distinct but chemically identical α-synuclein polymorphs. In ThT fluorescence assays the two polymorphs show type-specific fluorescence intensity behaviour although their β-sheet content has been shown to be similar. Further, fluorescence lifetime measurements of fibril-bound ThT reveal the presence of at least two qualitatively different ThT binding sites on the polymorphs. The relative distributions of the binding sites on the fibril surfaces appear to be morphology dependent, thus determining the observed polymorph-specific ThT fluorescence intensities. These results, highlighting the role of fibril morphology in ThT-based amyloid studies, underline the relevance of polymorphs in ThT–amyloid interaction and can explain the variability often observed in ThT amyloid binding assays.

Abbreviations: AFM: atomic force microscopy; AD: Alzheimer's disease; αSyn: α-synuclein; A30P: alanine at position 30 mutated to proline; A53T: alanine at position 53 mutated to threonine; EM: electron microscopy; HD: Huntington's disease; PD: Parkinson's disease; RSP: residual soluble protein; TCSPC: time correlated single photon counting; ThT: Thioflavin-T

ARTICLE HISTORY
Received 20 April 2018
Revised 19 July 2018
Accepted 27 August 2018

KEYWORDS
Amyloid; polymorphism; α-synuclein; thioflavin-T; atomic force microscopy

Introduction

In vitro fibrillization of recombinantly produced proteins is frequently used as the first step to understand the physicochemical properties of amyloid proteins associated with a number of neurodegenerative diseases, like Alzheimer's disease (AD), Parkinson's disease (PD), or Huntington's disease (HD) [1]. Amyloid formation in *in vitro* experiments is usually probed by thioflavin-T (ThT) based fluorescence assays [2]. The ThT fluorescence intensity shows an amyloid-specific enhancement upon binding to cross-β-sheet containing fibrils. Despite the prevalent use of ThT for amyloid studies, observations like variability in ThT fluorescence intensities between replicates and the factors influencing amyloid fibril–ThT interactions are not well understood.

ThT is a cationic benzothiazole molecule, proposed to behave as a molecular rotor. In solution, the benzylamine and benzathiole rings of ThT can freely rotate about their shared carbon–carbon bond leading to quenched fluorescence. On binding to the cross β-sheet structures of amyloid fibrils, the rotational freedom about the carbon–carbon bond is lost, resulting in a chiral twisted conformation, which impedes non-radiative decay and thus enhances the fluorescence [3–7]. ThT is suggested to bind as a monomer on the fibril surface, where amino acid side-chains form binding channels oriented parallel to the long axis of the fibrils [2–6,8,9]. ThT is reported to have multiple binding sites on a fibril with comparable or distinct binding affinities [7,9–12]. Studies on amyloid $\beta_{1\text{-}40}$ ($A\beta_{1\text{-}40}$) and lysozyme fibrils suggested the presence of three and two high affinity binding sites respectively, with different binding stoichiometries [11–13]. Further, simulation studies on amyloid fibril–ThT interactions indicate a preference for spatially consecutive aromatic (tyrosine and phenylalanine) and hydrophobic (valine and leucine) amino acids in the binding channels as opposed to charged residues, thus suggesting a sequence-based determinant of ThT binding [14,15]. It is well known that single amino acid differences in amyloidogenic proteins can influence the aggregation behaviour, the

CONTACT Ine Segers-Nolten g.m.j.segers-nolten@utwente.nl; Arshdeep Sidhu a.sidhu@erasmusmc.nl Nanobiophysics, MESA + Institute for Nanotechnology, University of Twente, P.O. Box 217, AE Enschede 7500, The Netherlands
*Present address: Department of Molecular Genetics, Erasmus MC, P.O. Box 2040, 3000 CA, Rotterdam, The Netherlands

Supplemental data for this article can be accessed here.

structure and morphology of the fibrils produced [16–19]. Moreover, the self-assembly of a single type of protein monomer or peptide may result in a variety of fibril morphologies, known as polymorphism. For the Aβ peptide, polymorphism as observed in atomic force microscopy (AFM) and electron microscopy (EM) [20] studies was reported to arise primarily from conformational variations in non-β-strand segments in the monomers when incorporated in the fibrils [21,22]. These conformational differences are likely to result in altered boundaries of the β-strand segments in the folded monomers and in different quaternary interactions between the protofilaments [21,23]. This implies that fibrils with distinct morphologies can have characteristic surface features, exposing different types of binding sites for interaction with amyloid-binding compounds like ThT, thus determining the fluorescence emitted by fibril-bound ThT [24,25].

In the present study, we investigate the relation between fibril morphology, ThT fluorescence behaviour and ThT binding sites. We use recombinantly produced α-synuclein (αSyn), linked to the pathogenesis of PD, as a model protein and compare the ThT fluorescence intensity in two polymorphs formed by two disease associated mutants, A30P (alanine at position 30 mutated to proline) and A53T (alanine at position 53 mutated to threonine). A30P and A53T αSyn form ThT-positive fibrils with characteristic aggregation kinetics and fibril morphologies (polymorphs). By seeded aggregation reactions, we prepared fibrils with identical wild-type (wt) monomers templated on low concentrations of A30P or A53T seeds that produced fibrils with high chemical similarity (99.98% wt monomers). The resultant fibrils exhibited the fibril–ThT interaction typical of the parent polymorphs. Further insights from the residual soluble protein (RSP) concentrations and the fluorescence lifetimes of ThT when bound to the two polymorphs at room temperature and 80 °C revealed that morphologically discrete fibrils have at least two qualitatively distinct binding sites for ThT on their surface. Moreover, the distribution of these sites on the fibril surface, a consequence of the fibril morphology, determines the observed ThT fluorescence intensity.

Materials and methods

αSyn purification and fibrillization

Wt and two disease associated mutants of αSyn (A30P and A53T) were expressed and purified as described earlier [26]. A30P and A53T were fibrillized in a *de novo* aggregation reaction as follows: 250 μM monomeric stocks, frozen at −80 °C were thawed and fibrillized in reactions with 100 μM αSyn, 10 mM Tris-HCl, 10 mM NaCl, 0.1 mM EDTA, and 20 μM ThT, at pH 7.4. The fibrils produced in the aggregation reaction were termed F_0 generation. All the reactions were prepared in triplicates in 200 μl volume and incubated in 96-well plates with optical bottoms (non-treated-Optical Polystyrene Polymer Bottom plates, Nunc, Thermo Fisher Scientific (Waltham, MA), Cat # 265301), sealed with adhesive film (Viewseal, Greiner Bio One, St. Louis, MO). The plates were incubated at 37 °C with orbital shaking in a Safire2 microplate reader (Tecan, Männedorf, Switzerland) for 96 h. The aggregation reactions were monitored by using 446 nm excitation and by following the ThT fluorescence emission intensity (bottom reading) at 485 nm. Readings were taken every 15 min.

Seeded aggregation reactions

Seeded aggregation reactions were performed using preformed fibrils as seeds. Seeds were prepared by sonicating 100 μl of A30P and A53T fibrils (from generation F_0) in a bath sonicator (Branson 1510) for 2 min in thin walled 200 μl PCR tubes. Aggregation reactions were set up as mentioned above but with 98 μM wt αSyn monomers and 2 μM seeds (based on initial monomer concentration) of A30P and A53T fibrils (from generation F_0). Fibrillization was followed as previously stated (resultant fibrils: F_1). Next, the fibrils formed in the F_1 generation were used as seeds (1 μM) following the same protocol as above to produce F_2 generation fibrils. The fibrils produced in the F_1 and F_2 generations are called as A30P and A53T templated fibrils based on the seeds used from the F_0 aggregation reaction (for a schematic representation of the strategy refer to Supporting information Figure S1).

Atomic force microscopy (AFM)

AFM samples were prepared at the end phase of each aggregation reaction (as determined by the ThT assay) to compare the morphology of the formed fibrils. The samples were prepared by about 10-fold dilution of the aggregation reactions in aggregation buffer. The samples (10 μl) were adsorbed on freshly cleaved mica (Muscovite, V-1 quality, EMS) for 4 min, followed by gentle washing with 100 μl of Milli-Q water and drying in a mild stream of N_2 gas (filtered through a 0.22 μm filter). AFM images were acquired on a Bioscope Catalyst instrument (Bruker, Billerica, MA) in soft tapping mode in air using a NSC36 probe, tip B, with a force constant of 1.75 N/m (NanoAndMore). All images were captured with a resolution of 512 × 512 pixels per image at a scan rate of 0.5 Hz. Post-acquisition, images were processed using Scanning Probe Image Processor (SPIP) 6.0.13 software (Image Metrology, Boston, MA).

Residual soluble protein (RSP) concentration determination

To determine the amount of soluble protein in the aggregation reaction at the plateau phase (as determined by the ThT assay), 100 μl of aggregation reaction mix was centrifuged at 21,000 × *g* at room temperature for 1 h in an IEC Micromax microcentrifuge (Thermo Fisher Scientific, Waltham, MA). Fifty microliters of the supernatant were removed and the absorbances, A_{280} and A_{330} at 280 and 330 nm, respectively, were measured on a NanoDrop ND-1000 spectrophotometer (Isogen Life Science, De Meern, The Netherlands). The absorption at 280 nm was corrected for scattering contributions (A_{330}), possibly from oligomeric

assemblies, before calculation of the RSP concentration [27]. The residual concentration of ThT was calculated by measuring the absorbance of the supernatant at 412 nm and using an extinction coefficient of 26,620 cm^{-1} M^{-1}.

ThT fluorescence lifetime measurements

The fluorescence lifetimes of ThT when bound to A30P and A53T templated fibrils (F_2) were determined by analysis of the fluorescence decay curves obtained by time correlated single photon counting (TCSPC). TCSPC measurements were done on a single photon-counting controller FluoroHub connected to a Fluoromax-4 spectrofluorometer (HORIBA Jobin Yvon, Clifton Park, NY). The instrument response function (prompt) was measured by illumination of a Ludox AS-30 colloidal silica solution at 460 nm. A pulsed diode light source, NanoLED-460 nm with a pulse duration of 1.3 ns and a repetition rate of 1 MHz was used for illumination (slit width: 5 nm). Next, the samples were illuminated with the same source and the emission was followed at 485 nm in a 5 mm path length quartz cuvette. The decay curves were analyzed using DAS6 software (HORIBA Jobin Yvon, Clifton Park, NY), which uses reconvolution of the instrument response function to accurately recover the samples' decay. A 2-component exponential fit was used to obtain the lifetimes of the fast and slow components along with their relative amplitudes.

Results and discussion

A30P and A53T αSyn are two disease associated mutants of αSyn implicated in familial forms of Parkinson's disease. The two mutants have been shown to exhibit distinct aggregation kinetics and fibril morphologies [17–19,28–30]. In earlier studies, we have shown that these disease mutants form stable fibrils of distinct morphology and that cross seeded aggregation between these mutants is sensitive for seed morphology [19,30]. Based on these observations, we here study the interaction of morphologically distinct but chemically identical polymorphs of αSyn with the standard amyloid probe ThT, to understand the contribution of fibril morphology in ThT readouts.

αSyn polymorphs from A30P and A53T monomers

A30P and A53T monomers were fibrillized in uniform aggregation conditions with 20 μM ThT. Titration of 100 μM αSyn fibrils (wt-F_0, A30P templated-F_2 and A53T templated-F_2) against ThT showed a sharp increase in ThT fluorescence intensity up till about 20 μM ThT concentration followed by a gradual decrease in the fluorescence intensity (Figure S2) (note 1 in SI; Figure S3) [31]. Therefore, 20 μM ThT was chosen to follow all the aggregation reactions. The $t_{1/2}$ for A30P aggregation was ~36 h, while $t_{1/2}$ for A53T aggregation was ~20 h, showing faster aggregation of A53T monomers in comparison to A30P monomers. A30P fibrils exhibited higher final fluorescence intensity in comparison to A53T fibrils at the plateau phase (Figure 1(A)). The plateau phase aggregation reactions are typically a mix of fibrils, oligomers and monomers. Monomers and oligomers do not usually result in an increase in the ThT fluorescence (Figure S4), therefore the majority of the enhanced ThT fluorescence is expected from fibril–ThT interaction. To determine the concentration of protein in fibrillar form, contributing to the enhanced ThT fluorescence intensity, fibrils were separated from monomers and oligomers by high-speed centrifugation. Surprisingly, the RSP concentration showed greater conversion of soluble monomers into fibrils in the A53T aggregation reaction compared to the A30P aggregation reaction (Figure 2: F_0 and Table S1). Thus, the RSP concentration determination and fluorescence intensities show that a lower fibril mass of A30P fluoresces with higher intensity than a higher mass of A53T fibrils.

Next, the fibrils from the plateau phase were imaged by tapping mode AFM to study the fibril morphology. Extensive quantitative morphological studies, over a period of one year, have been reported previously by our group for

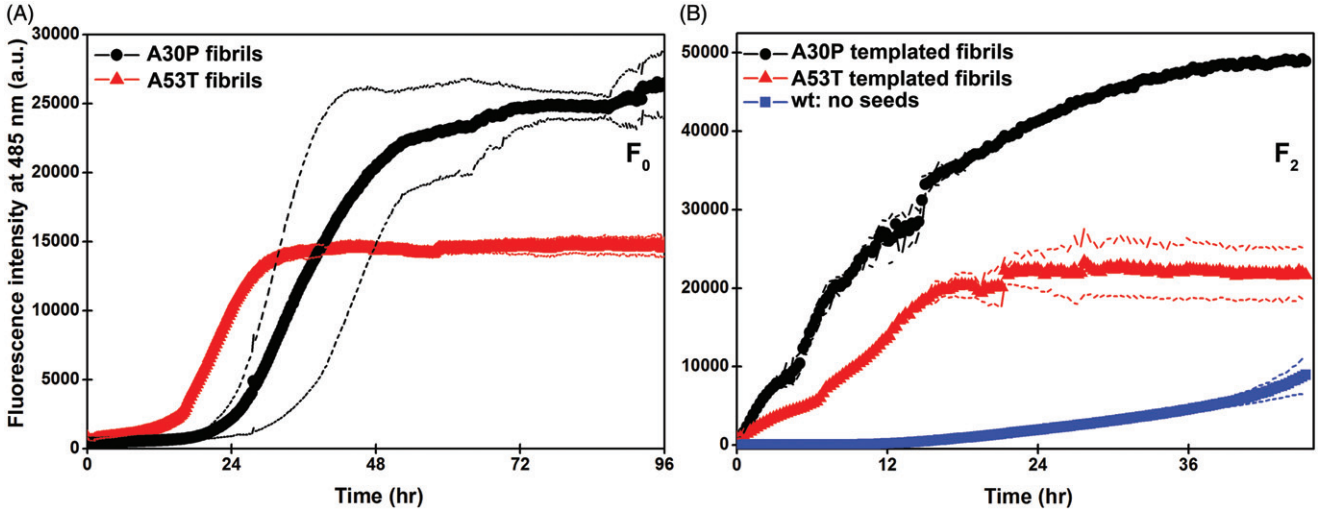

Figure 1. ThT aggregation kinetics for (A) unseeded A30P and A53T monomers (F_0 generation) and (B) seeded aggregation with wt monomers and A30P and A53T templating seeds (F_2 generation). Dashed lines around the curves denote standard deviation among the triplicates.

A30P and A53T fibrils [30]. Here, A30P and A53T samples contained several micron long fibrils (Figure 3(A,B): inset). AFM height images show A30P fibrils to have a periodic twist with an average periodicity (Figure 3(A,C)) in agreement with the previously reported average periodicity of 105 ± 7 nm and average height of 5.6 ± 0.7 nm [30]. The morphology of the A53T fibrils with longer periodicity and a number of fibrils associated with each other (heterogeneous fibrils) was also in accordance with the earlier reported average periodicity of 282 ± 87 nm along with heterogeneous fibrils and an average height of 6.4 ± 1.2 nm (Figure 3(B)) [30]. Thus, both the disease mutants formed fibrils of different morphology in the aggregation conditions used here. The inverse relation between ThT intensities and fibrillar mass, together with the apparent morphological differences suggest that ThT is likely to experience distinct binding surfaces on morphologically discrete fibrils, thereby affecting its fluorescence intensity.

The proposed polymorph-specific ThT interactions could arise due to characteristic secondary, tertiary, or quaternary fibril structure induced by the primary sequence (chemistry) of the αSyn monomers. However, we have previously shown using ATR-FTIR that even with distinct morphology, A30P and A53T fibrils have highly similar β-sheet content of 66% and 68%, respectively [30]. Moreover, recent high-resolution studies using solid-state NMR on polymorphic fibrils of β-endorphin fibrils reported nearly identical atomic structure in polymorphs [32]. Therefore, the morphological differences of the polymorphs are likely tertiary and/or quaternary in origin.

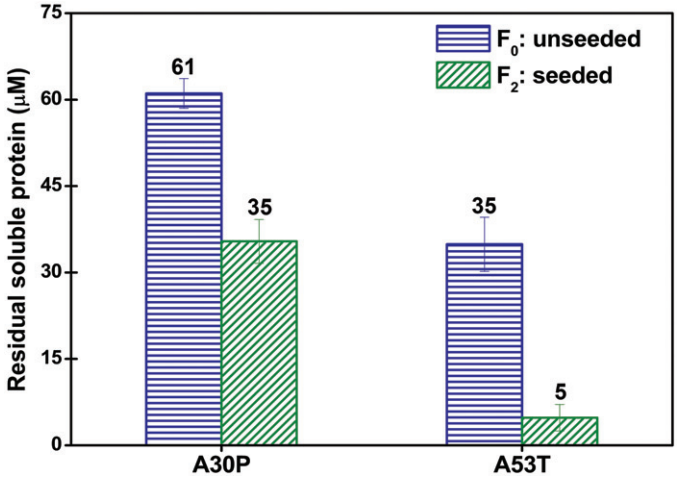

Figure 2. Residual soluble protein concentration of unseeded and seeded aggregation reactions.

Chemically identical wt αSyn polymorphs

The polymorphs from A30P and A53T monomers differ in two amino acids with respect to each other. To establish if the polymorph type-specific ThT fluorescence intensities are due to differences in the protein sequence and/or fibril morphology, we prepared chemically highly similar (99.98% wt monomers) but morphologically different fibrils by seeding wt monomers with A30P or A53T seeds. Aggregations were done for two generations with 2 μM (F_0 fibrils) and 1 μM (F_1 fibrils) seeds, respectively (Figure S1). Since the disease mutant protein contribution in the final aggregation reactions (F_2) is negligible (about 0.02%), we considered these fibrils to be chemically identical. The morphology of the resultant fibrils from each generation was probed by AFM to ascertain the preservation of seed (F_0) morphology over multiple aggregation reactions.

Morphology of chemically identical polymorphs

In our study, A30P seeded aggregation reactions produced fibrils with A30P fibril morphology, while A53T seeded aggregation reactions resulted in fibrils of A53T fibril morphology (Figure 4(A,B) and Figures S5 and S6). The transmission of seed morphology to wt αSyn monomers is in agreement with a previous seeded aggregation study [33]. The fibrils from A30P and A53T seeded aggregations will be subsequently referred to as A30P and A53T templated fibrils, respectively. The next round of seeded aggregation

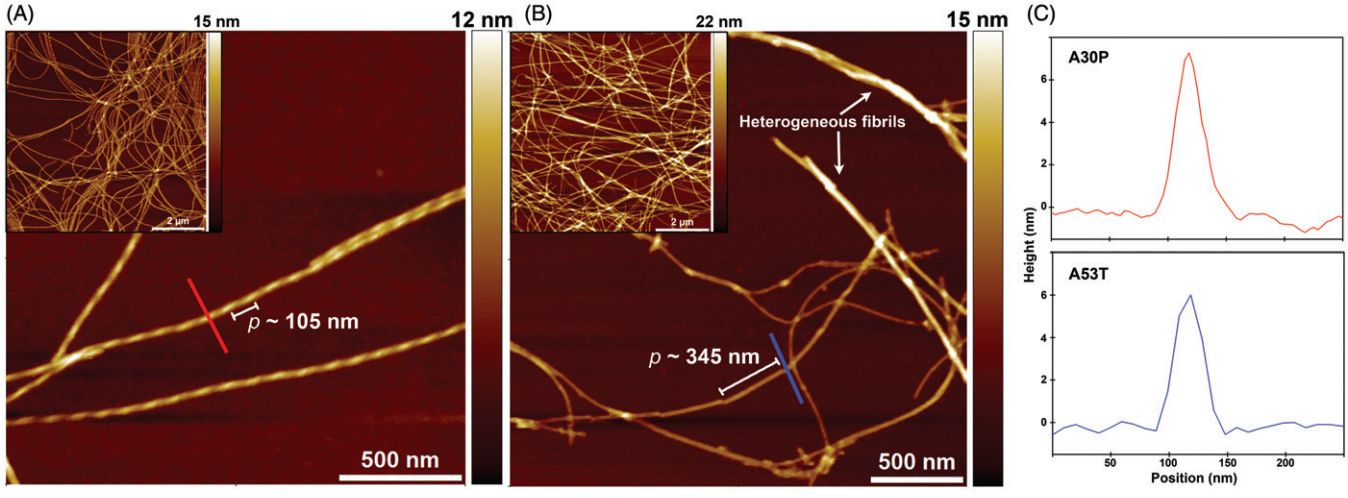

Figure 3. AFM height images of A30P (A) and A53T (B) fibrils at plateau phase. Inset: overview images showing dense and long fibrils in both samples. White labels show the length of representative periodic twist in respective fibrils. (C) Height cross-section of fibrils, A30P and A53T, at positions marked by cross-sectional lines in images (A and B).

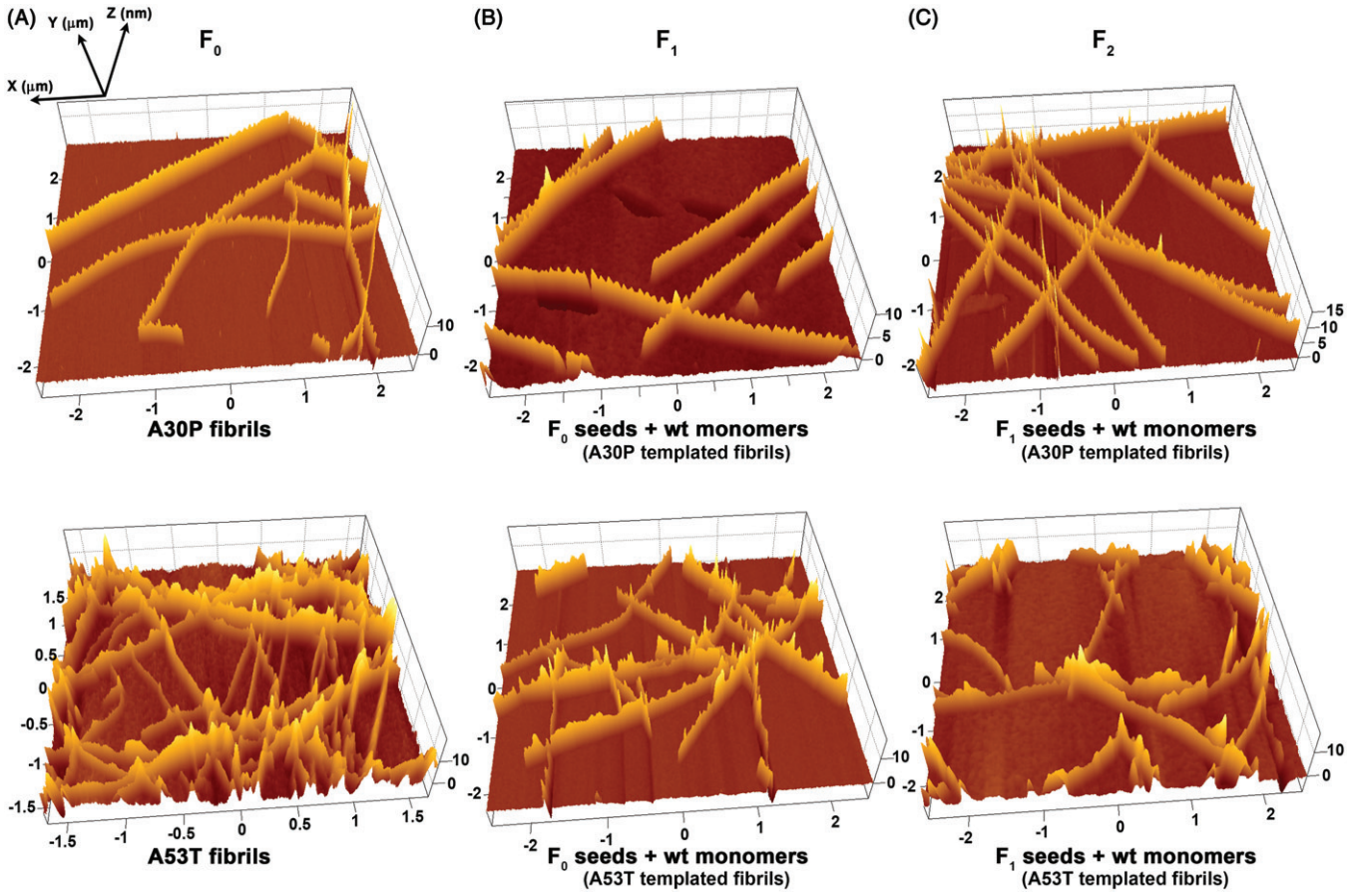

Figure 4. Representative AFM height images showing morphological templating by seeds in seeded aggregation reactions over two generations. For corresponding 2D AFM images, see Figures S5 and S6.

reaction (F_2) was performed with wt αSyn monomers, using A30P and A53T templated fibrils from the F_1 generation as seeds. The fibrils produced (F_2 generation) recapitulated the fibril morphologies of the seeds with average periodicity of 113 ± 6 nm ($N = 49$) for A30P templated fibrils and 262 ± 67 nm ($N = 34$) for A53T templated fibrils (Figure 4(C) and Figures S5 and S6). The A53T templated fibrils also showed heterogeneous and non-periodic fibrils that are characteristic of A53T fibrils [30]. Therefore, at the plateau phase of the F_2 generation, both types of fibrils (A30P and A53T templated) are composed of the same monomers (wt αSyn) but exhibit different morphologies, characteristic of A30P and A53T fibrils in F_0 (Figure 4 and Figures S5 and S6).

ThT aggregation kinetics of chemically identical polymorphs

As expected, with seeded aggregation reactions, the fibrillization kinetics of A30P and A53T templated fibrils, based on the ThT intensity assay, did not show a lag phase in both F_1 and F_2 generation. In seeded aggregation reactions with A30P as well as A53T templated fibrils, the $t_{1/2}$ was ~12 h. A30P templated fibrils showed higher fluorescence intensity compared with the A53T templated fibrils from the start, and akin to the F_0 generation had higher final fluorescence intensity (F_2 shown in Figure 1(B)). The RSP concentration however revealed incorporation of 95% of the monomers into fibrils in A53T templated fibrils as opposed to only 65% in A30P templated fibrils (Figure 2: F_2 and Table S1) which showed more intense ThT emission. We checked the supernatants for the presence of residual fibrillar aggregates by ThT assays. None of the samples showed an increase in the fluorescence intensity, thus indicating that ThT positive aggregates are not present in the supernatant (data not shown). The lower fluorescence intensity of the A53T templated fibrils is also not due to less ThT binding as calculations based on residual ThT concentrations showed that all of the provided ThT was bound in the A53T templated fibrils (Table 1). The chosen concentration was also not limiting in the aggregation reactions as addition of additional (20 μM) ThT at the end of the aggregation reactions did not result in higher fluorescence intensity (data not shown). Therefore, in comparison to A53T templated fibrils, lower fibrillar mass of A30P templated fibrils shows distinctly higher fluorescence intensity with a

Table 1. ThT to protein binding ratios for F_2 generation fibrils (± stdv among triplicates).

	A30P templated fibrils	A53T templated fibrils
Monomers in fibrils	65 ± 4 μM	95 ± 2 μM
ThT bound	17 ± 2 μM	20 ± 0 μM
μM ThT/μM monomer	0.26	0.21

comparable fraction of bound ThT. Observation of the same trend, in both the ThT intensity assay and RSP concentrations, between the non-seeded (F_0) and seeded (F_2) fibrils (see Note 2 in SI) is in agreement with one of our previous reports where aggregation characteristics in a seeded aggregation reaction were reported to be seed-specific [19] and suggests that the ThT fluorescence intensity is related to the fibril morphology.

ThT fluorescence lifetimes and relative amplitudes

The observed trend in the ThT assay and RSP concentrations could be due to different types of binding sites that affect the quantum yield of the fibril bound ThT [7]. The simplest explanation could be that the fluorescence quantum efficiency of ThT bound to A30P templated fibrils is higher than when bound to A53T templated fibrils, which results in higher fluorescence. To probe this hypothesis, we measured the fluorescence lifetimes (higher quantum efficiency should give longer lifetime) of ThT in A30P and A53T templated fibrils (F_2) by time correlated single photon counting (TCSPC). The fluorescence decay curves for A30P and A53T templated fibrils did not show a single exponential decay signifying there is more than one type of binding site on the fibrils' surface. The data were analyzed with a 2-component exponential fit, which was found sufficient to fit the data accurately (Figure 5).

ThT bound to both polymorphs showed a fast (τ_1) and slow (τ_2) lifetime component (Table 2). The lifetime of the slow component when bound to A30P and A53T templated fibrils is not significantly different at 1.68 ± 0.02 and 1.64 ± 0.04 ns, respectively. The lifetime of the fast component of A30P templated fibrils and for A53T templated fibrils is also similar (0.31 ± 0.04 and 0.22 ± 0.01 ns, respectively). However, notably different values for τ_1 and τ_2 suggest that ThT binds to different binding sites that allow varied degree of intermolecular flexibility in bound ThT. τ_1 with lifetimes in the range of some hundred picoseconds, most likely corresponds to ThT sites that allow some intramolecular flexibility leading to low fluorescence. τ_2 with lifetimes in the nanosecond range, likely represents tight embedding of ThT molecules that hinders non-radiative deactivation. The relative amplitude of the slower component is 17 percentage points less in A53T (40%) than in A30P (57%) templated fibrils, suggesting that the proportion of these binding sites on the two polymorphs are different (Table 2). Therefore, the observed fluorescence intensity trends for ThT bound to fibrils of distinct morphology is not due to global differences in the fluorescence quantum efficiency but due to differences in the relative distribution of at least two ThT binding sites on the fibril surfaces.

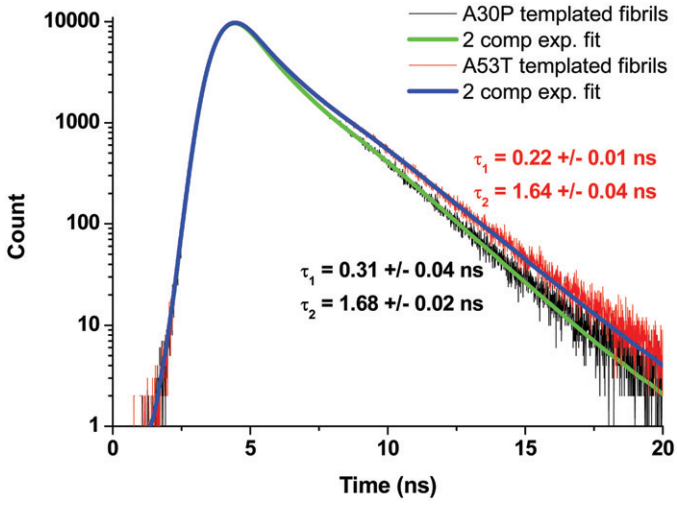

Figure 5. Representative fluorescence lifetime decay curves for A30P and A53T templated fibrils with the corresponding 2 component exponential fit at RT.

To gain further insights if the binding sites resulting in τ_1 and τ_2 in A30P and A53T templated fibrils are identical or different, we determined fluorescence lifetimes at 80 °C. At higher temperature, the dynamic equilibrium between the fibril–ThT interactions is expected to change due to temperature sensitive flexibility of the ThT-binding sites. Similar changes in the samples would suggest similar binding sites on the two types of fibrils.

At 80 °C, the lifetime of the slow component of ThT bound to A30P templated fibrils changed marginally from 1.68 ± 0.02 to 1.60 ± 0.04 ns, but the relative amplitude dropped by 35 percentage points from 57% to 22%. ThT bound to A53T templated fibrils on the other hand showed a 20% decrease in lifetime (1.30 ± 0.04 ns) as well as 18 percentage point decrease in the relative amplitude. Hence, at higher temperature, the changes in the fibril–ThT interactions are very different; this confirms that the binding sites for ThT on A30P and A53T templated fibrils are different.

The presence of different binding sites in polymorphs thus results in distinct ThT intensities. Therefore, aggregation reactions resulting in different relative ratios of polymorphs can be expected to show different final fluorescence intensities. Given the stochastic nature of nucleation and fibrillization, even within triplicates the ratio of polymorphs is expected to be different. Varied distribution of polymorphs in an aggregation reaction could thus be the likely explanation for the generally poor reproducibility of ThT based fluorescence assays. Congruently, as also shown in this report, seeded aggregation reactions and protocols

Table 2. Fluorescence lifetimes determined for ThT bound to A30P and A53T templated fibrils (F_2) at room temperature (RT) and 80 °C (± stdv among triplicates).

	A30P templated fibrils				A53T templated fibrils			
	Lifetimes (ns)		Amplitude (%)		Lifetimes (ns)		Amplitude (%)	
	τ_1	τ_2	1	2	τ_1	τ_2	1	2
RT	0.31 ± 0.04	1.68 ± 0.02	43 ± 3	57 ± 3	0.22 ± 0.01	1.64 ± 0.04	60 ± 5	40 ± 6
80 °C	0.12 ± 0.01	1.60 ± 0.04	78 ± 8	22 ± 8	0.13 ± 0.03	1.30 ± 0.04	78 ± 5	22 ± 5

optimized to yield homogeneous fibril populations, display improved reproducibility in ThT assays [26,34,35].

Conclusions

ThT is routinely used as a standard probe in comparative aggregation studies to examine the effect of mutations, solution conditions, and small molecule inhibitors on amyloid aggregation kinetics. Bulk aggregation reactions, however, normally contain a morphologically heterogeneous population of amyloid fibrils. We show from chemically identical polymorphs of αSyn that the distribution of qualitatively different binding sites is polymorph specific. In case of αSyn, polymorphs of A30P and A53T mutants present at least two ThT binding sites that allow different degrees of flexibility for the bound ThT molecule and consequently variable fluorescence intensities. Thus, modes of fibril–ThT interaction are highly specific for fibril morphology and the relative distributions of binding sites determine the observed ThT intensities.

Acknowledgements

The authors thank Kirsten van Leijenhorst-Groener, Yvonne Kraan and Nathalie Schilderink for protein expression and purification, and Dr Martin Bennink, Kees van der Werf and Robert Molenaar for advice on AFM.

Disclosure statement

No potential conflict of interest was reported by the authors.

Funding

This work is supported by NanoNextNL, a micro- and nanotechnology consortium of the Government of The Netherlands and 130 partners.

ORCID

Arshdeep Sidhu http://orcid.org/0000-0002-2851-1019

References

[1] Knowles TP, Vendruscolo M, Dobson CM. The amyloid state and its association with protein misfolding diseases. Nat Rev Mol Cell Biol. 2014;15:384–396.
[2] Groenning M. Binding mode of Thioflavin T and other molecular probes in the context of amyloid fibrils-current status. J Chem Biol. 2010;3:1–18.
[3] Biancalana M, Koide S. Molecular mechanism of Thioflavin-T binding to amyloid fibrils. Biochim Biophys Acta. 2010;1804:1405–1412.
[4] Kuznetsova IM, Sulatskaya AI, Maskevich AA. High fluorescence anisotropy of Thioflavin T in aqueous solution resulting from its molecular rotor nature. Anal Chem. 2016;88:718–724.
[5] Amdursky N, Erez Y, Huppert D. Molecular rotors: what lies behind the high sensitivity of the Thioflavin-T fluorescent marker. Acc Chem Res. 2012;45:1548–1557.
[6] Maskevich AA, Stsiapura VI, Kuzmitsky VA, et al. Spectral properties of Thioflavin T in solvents with different dielectric properties and in a fibril-incorporated form. J Proteome Res. 2007;6:1392–1401.
[7] Freire S, de Araujo MH, Al-Soufi W, et al. Photophysical study of Thioflavin T as fluorescence marker of amyloid fibrils. Dyes Pigments. 2014;110:97–105.
[8] Krebs MR, Bromley EH, Donald AM. The binding of thioflavin-T to amyloid fibrils: localisation and implications. J Struct Biol. 2005;149:30–37.
[9] Sulatskaya AI, Kuznetsova IM, Belousov MV, et al. Stoichiometry and affinity of Thioflavin T binding to Sup35p amyloid fibrils. PLoS One. 2016;11:e0156314.
[10] LeVine H. Quantification of beta-sheet amyloid fibril structures with Thioflavin T. Meth Enzymol. 1999;309:274–284.
[11] Sulatskaya AI, Kuznetsova IM, Turoverov KK. Interaction of thioflavin T with amyloid fibrils: fluorescence quantum yield of bound dye. J Phys Chem B. 2012;116:2538–2544.
[12] Sulatskaya AI, Kuznetsova IM, Turoverov KK. Interaction of Thioflavin T with amyloid fibrils: stoichiometry and affinity of dye binding, absorption spectra of bound dye. J Phys Chem B. 2011;115:11519–11524.
[13] Lockhart A, Ye L, Judd DB, et al. Evidence for the presence of three distinct binding sites for the thioflavin T class of Alzheimer's disease PET imaging agents on beta-amyloid peptide fibrils. J Biol Chem. 2005;280:7677–7684.
[14] Wu C, Biancalana M, Koide S, et al. Binding modes of Thioflavin-T to the single-layer beta-sheet of the peptide self-assembly mimics. J Mol Biol. 2009;394:627–633.
[15] Wu C, Wang Z, Lei H, et al. Dual binding modes of Congo red to amyloid protofibril surface observed in molecular dynamics simulations. J Am Chem Soc. 2007;129:1225–1232.
[16] Heise H, Celej MS, Becker S, et al. Solid-state NMR reveals structural differences between fibrils of wild-type and disease-related A53T mutant alpha-synuclein. J Mol Biol. 2008;380:444–450.
[17] Conway KA, Harper JD, Lansbury PT. Accelerated in vitro fibril formation by a mutant alpha-synuclein linked to early-onset Parkinson disease. Nat Med. 1998;4:1318–1320.
[18] van Raaij ME, Segers-Nolten IM, Subramaniam V. Quantitative morphological analysis reveals ultrastructural diversity of amyloid fibrils from alpha-synuclein mutants. Biophys J. 2006;91:L96–L98.
[19] Sidhu A, Segers-Nolten I, Subramaniam V. Conformational compatibility is essential for heterologous aggregation of alpha-synuclein. ACS Chem Neurosci. 2016;7:719–727.
[20] Qiang W, Kelley K, Tycko R. Polymorph-specific kinetics and thermodynamics of β-amyloid fibril growth . J Am Chem Soc. 2013;135:6860–6871.
[21] Paravastu AK, Leapman RD, Yau WM, et al. Molecular structural basis for polymorphism in Alzheimer's beta-amyloid fibrils. Proc Natl Acad Sci USA. 2008;105:18349–18354.
[22] Lu JX, Qiang W, Yau WM, et al. Molecular structure of β-amyloid fibrils in Alzheimer's disease brain tissue . Cell. 2013;154:1257–1268.
[23] Gath J, Bousset L, Habenstein B, et al. Unlike twins: an NMR comparison of two alpha-synuclein polymorphs featuring different toxicity. PLoS One. 2014;9:e90659.
[24] Lindberg DJ, Wranne MS, Gilbert Gatty M, et al. Steady-state and time-resolved Thioflavin-T fluorescence can report on morphological differences in amyloid fibrils formed by Abeta(1-40) and Abeta(1-42). Biochem Biophys Res Commun. 2015;458:418–423.
[25] Nielsen SB, Macchi F, Raccosta S, et al. Wildtype and A30P mutant alpha-synuclein form different fibril structures. PLoS One. 2013;8:e67713.
[26] Sidhu A, Segers-Nolten I, Subramaniam V. Solution conditions define morphological homogeneity of alpha-synuclein fibrils. Biochim Biophys Acta. 2014;1844:2127–2134.

[27] Grimsley GR, Pace CN. Spectrophotometric determination of protein concentration. Curr Protoc Protein Sci. 2004. DOI: 10.1002/0471140864.ps0301s33
[28] Giasson BI, Uryu K, Trojanowski JQ, et al. Mutant and wild type human alpha-synucleins assemble into elongated filaments with distinct morphologies in vitro. J Biol Chem. 1999;274: 7619–7622.
[29] Narhi L, Wood SJ, Steavenson S, et al. Both familial Parkinson's disease mutations accelerate alpha-synuclein aggregation. J Biol Chem. 1999;274:9843–9846.
[30] Sidhu A, Segers-Nolten I, Raussens V, et al. Distinct mechanisms determine alpha-synuclein fibril morphology during growth and maturation. ACS Chem Neurosci. 2017;8:538–547.
[31] Xue C, Lin TY, Chang D, et al. Thioflavin T as an amyloid dye: fibril quantification, optimal concentration and effect on aggregation. R Soc Open Sci. 2017;4:160696.
[32] Seuring C, Verasdonck J, Ringler P, et al. Amyloid fibril polymorphism: almost identical on the atomic level, mesoscopically very different. J Phys Chem B. 2017;121: 1783–1792.
[33] Bousset L, Pieri L, Ruiz-Arlandis G, et al. Structural and functional characterization of two alpha-synuclein strains. Nat Commun. 2013;4:2575.
[34] Buell AK, Galvagnion C, Gaspar R, et al. Solution conditions determine the relative importance of nucleation and growth processes in alpha-synuclein aggregation. Proc Natl Acad Sci USA. 2014;111:7671–7676.
[35] Meisl G, Yang X, Dobson CM, et al. Modulation of electrostatic interactions to reveal a reaction network unifying the aggregation behaviour of the Abeta42 peptide and its variants. Chem Sci. 2017;8:4352–4362.